Program Digest, 2019 IEEE International Ultrasonics Symposium (IUS)
Glasgow, Scotland, October 6-9, 2019

Perturbation Analysis of Nonlinearity in Radio Frequency Bulk Acoustic Wave Resonators Using Mass-Spring Model

Ken-ya Hashimoto[1,2], Xinyi Li[2,1], Jingfu Bao[2], Luyan Qiu[1], and Tatuya Omori[1]
[1]Graduate School of Engineering, Chiba University, Chiba 263-8522, Japan
[2]School of Electronic Engineering, University of Electronic Science and Technology of China, Chengdu 611737, China
E-mail: k.hashimoto@ieee.org

Abstract— **This paper describes derivation of an equivalent circuit for nonlinear responses in film bulk acoustic resonators from the first-order perturbation analysis using the piezoelectric constitutive equations with the *h*-form. For simplicity, electrodes and piezoelectric layer are regarded as a mass and spring in the derivation. Then it is demonstrated that the H2 response can be simulated well by the circuit.**

I. Introduction

Advance in mobile communications requests further suppression of nonlinear signal generation in radio frequency (RF) surface and bulk acoustic wave (SAW/BAW) resonators[1-4]. For the purpose, accurate and fast simulation tools are demanded.

Shim and Feld proposed an nonlinear equivalent circuit for the purpose[2]. In the analysis, multiple nonlinearities are included simultaneously, and the nonlinear response is analyzed by the harmonic balance method[5].

Since nonlinearity in RF SAW/BAW devices is weak, the first-order perturbation analysis should be enough. The authors indicated that non-linear behaviors of RF BAW resonators are simulated well in high speed by the first-order perturbation analysis in combination of the piezoelectric constitutive equations with the *h* form instead of those with the *e* form[6].

The authors also applied the perturbation analysis to the two dimensional (2D) case, and demonstrated that H2 behavior including transverse modes can be explained well by a first-order 2D perturbation analysis[7]. However, these analyses were based on the wave equations, it is not convenient to understand nonlinear behaviors intuitively although the simulation is very fast.

This paper describes derivation of a 1D nonlinear equivalent circuit from the perturbation analysis based on the constitutive equations with the *h* form.

To simply the derivation, the following approximations are applied.

1. Electrodes are very heavy and stiff, and their deformation is negligible.
2. The piezo layer is very light, and its inertia (mass) is negligible.

Namely, electrodes and piezo layer are regarded as simple two masses and a spring, respectively. The mass-spring model stands for current FBAR structures employing heavy and stiff electrodes for enhancing the effective electromechanical coupling factor[8].

II. Modelling of Thickness Resonator

A. *Linear Analysis*

Let us apply 1D analysis to a thickness resonator shown in Fig. 1, which is composed of a piezoelectric layer with the thickness L sandwiched in between two electrodes with the thickness l. Here we assume the electrode width W is much larger than L and l, and the electrode area A is given by W^2.

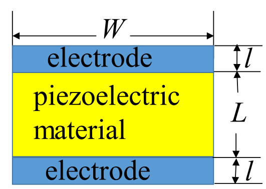

Fig. 1 Thickness resonator configuration used in this analysis

Fields in the piezoelectric body are assumed to be governed by the following linear constitutive equations with the h form:

$$T = c^D S - hD\,, \tag{1}$$

and

$$E = \beta^S D - hS\,, \tag{2}$$

where T, S, D, and E are stress, strain, electric flux density, and electric field, respectively, c^D is the stiffness under constant D, β^S is the inverse permittivity under constant S, and h is the piezoelectric constant.

The electric current I flowing to the top electrode is given by

$$D = \frac{jI}{\omega A}\,, \tag{3}$$

and the conservation law of the flux density is given by

$$\frac{\partial D}{\partial x} = 0\,. \tag{4}$$

978-1-7281-4595-2/19/$31.00 ©2019 IEEE

Eq. (4) indicates that D is independent of x, namely uniform. The mass-spring model indicates that S is also independent of x. Thus that the voltage V between two electrodes is given by

$$V=-\int_{-L/2}^{L/2} E dx=-L\left[\beta^{\mathrm{S}} D-hS\right]. \tag{5}$$

from Eq. (2). On the other hand, one may obtain the following equation of motion from Eq. (1):

$$-\rho\omega^2 lu+c^{\mathrm{D}} S-hD=0, \tag{6}$$

where ρ is the mass density of the electrodes, and u is the displacement of the top electrode. When we set u=0 at the center of the piezo-layer, u is given by $SL/2$. Then Eq. (6) gives

$$S=\frac{hD}{c^{\mathrm{D}}-\rho\omega^2 lL/2}=\frac{h/c^{\mathrm{D}}}{1-(\omega/\omega_{\mathrm{a}})^2}\left(-\frac{I}{j\omega A}\right), \tag{7}$$

where ω_a is the anti-resonance frequency given by $(2c^D/\rho lL)^{0.5}$. Substitution of Eq. (7) to Eq. (5) gives

$$Y=\frac{I}{V}=j\omega C_0+\frac{j\omega C_0 k_{\mathrm{t}}^2}{1-k_{\mathrm{t}}^2-(\omega/\omega_{\mathrm{a}})^2}, \tag{8}$$

where C_0 is the clamped capacitance given by $\beta^{S-1}A/L$, and k_t^2 is the electromechanical coupling factor for the thickness vibration given by $h^2/c^D\beta^S$. Eq. (8) indicates that the resonance frequency ω_r is given by $\omega_a(1-k_t^2)^{0.5}$.

Eq. (8) gives an equivalent circuit shown in Fig. 2 for linear vibration[9], where $C_m=C_0/(k_t^{-2}-1)$ and $L_m=1/\omega_a^2C_0k_t^2$ are motional capacitance and inductance, respectively, and relations of $\omega_r=(L_mC_m)^{-0.5}$ and $\omega_a=\{L_m(C_0^{-1}+C_m^{-1})^{-1}\}^{-0.5}$ hold.

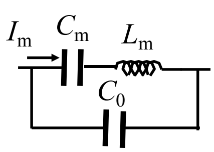

Fig. 2 Linear equivalent circuit

Modification of Eq. (8) gives a mechanical current I_m defined in Fig. 2 as

$$I_{\mathrm{m}}=\frac{k_{\mathrm{t}}^2}{1-(\omega/\omega_{\mathrm{a}})^2} I, \tag{9}$$

and its comparison with Eq. (7) gives

$$S=\frac{jh}{\omega A c^{\mathrm{D}} k_{\mathrm{t}}^2} I_{\mathrm{m}}=\frac{j\beta^{\mathrm{S}}}{\omega h A} I_{\mathrm{m}}. \tag{10}$$

When various loss mechanisms are introduced, one may obtain the modified BVD model[10] given in Fig. 3.

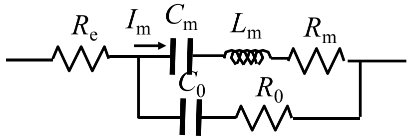

Fig. 3 Linear equivalent circuit including loss terms (Modified BVD model[10])

B. *Nonlinear analysis*

Let us introduce non-linear terms to the constitutive equations given in Eqs. (1) and (2), namely

$$T=c^{\mathrm{D}} S-hD+T_{\mathrm{N}} \tag{11}$$

and

$$E=\beta^{\mathrm{S}} D-hS+E_{\mathrm{N}}, \tag{12}$$

where T_N and E_N are the stress and electric field generated by nonlinearity. Substitution of Eqs. (11) and (12) to Eqs. (5) and (7) gives

$$V_{\mathrm{N}}=-L\left[\beta^{\mathrm{S}} D_{\mathrm{N}}-hS_{\mathrm{N}}\right]-LE_{\mathrm{N}} \tag{13}$$

and

$$S_{\mathrm{N}}=\frac{hD_{\mathrm{N}}-T_{\mathrm{N}}}{c^{\mathrm{D}}\left\{1-(\omega_{\mathrm{N}}/\omega_{\mathrm{a}})^2\right\}}. \tag{14}$$

Here the subscript N added to ω, V and I indicates that they are caused by nonlinearity. One may obtain the following relation after substitution of Eq. (14) to Eq. (13) and mathematical manipulation:

$$V_{\mathrm{N}}+LE_{\mathrm{N}}+\frac{k_{\mathrm{t}}^2\left(V_{\mathrm{N}}+LE_{\mathrm{N}}+\beta^{\mathrm{S}} Lh^{-1} T_{\mathrm{N}}\right)}{1-k_{\mathrm{t}}^2-(\omega_{\mathrm{N}}/\omega_{\mathrm{a}})^2}=-L\beta^{\mathrm{S}} D_{\mathrm{N}}. \tag{15}$$

Since $D_N=jI_N/\omega_N A$, one may obtain

$$I_{\mathrm{N}}=j\omega_{\mathrm{N}} C_0\left[V_{\mathrm{N}}+LE_{\mathrm{N}}\right] +\frac{j\omega_{\mathrm{N}} C_0 k_{\mathrm{t}}^2}{1-k_{\mathrm{t}}^2-(\omega_{\mathrm{N}}/\omega_{\mathrm{a}})^2}\left[V_{\mathrm{N}}+LE_{\mathrm{N}}+\frac{\beta^{\mathrm{S}} L}{h} T_{\mathrm{N}}\right]. \tag{16}$$

Eq. (16) gives the equivalent circuit model given in Fig. 4, where V_{NE}=$-LE_N$ and V_{NT}=$-\beta^S LT_N/h$ are voltage sources with the frequency of ω_N.

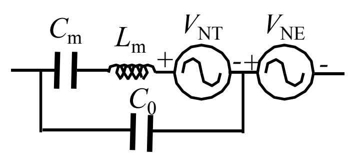

Fig. 4 Equivalent circuit including signal sources caused by nonlinearity

Introduction of loss mechanisms gives the equivalent circuit shown in Fig. 5.

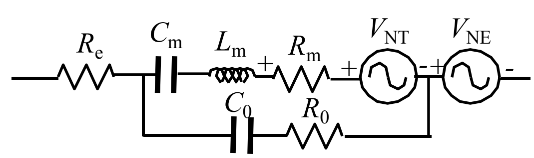

Fig. 5 Equivalent circuit including loss terms and signal sources caused by nonlinearity

Nonlinear responses are analyzed by the following steps.

First, peripheral circuits are added to the Modified BVD model given in Fig. 3, and I and I_m are calculated. Eqs. (3) and

(9) are used to estimate D and S from these values. Note that this analysis should be performed at two driving frequencies for evaluation of the inter-modulation distortion (IMD).

Next, T_{N} and E_{N} are estimated. Expansion of the Gibbs free energy until the third-order [11] gives nonlinear terms in the constitutive equations (11) and (12) to the following forms:

$$\begin{aligned} T_{\mathrm{N}} = & -\frac{1}{2}\chi_{20}^{\mathrm{T}}S^2 - \chi_{11}^{\mathrm{T}}SD - \frac{1}{2}\chi_{02}^{\mathrm{T}}D^2 \\ & -\frac{1}{6}\chi_{30}^{\mathrm{T}}S^3 - \frac{1}{2}\chi_{21}^{\mathrm{T}}S^2D - \frac{1}{2}\chi_{12}^{\mathrm{T}}SD^2 - \frac{1}{6}\chi_{03}^{\mathrm{T}}D^3 \end{aligned} \quad (17)$$

and

$$\begin{aligned} E_{\mathrm{N}} = & -\frac{1}{2}\chi_{11}^{\mathrm{T}}S^2 - \chi_{02}^{\mathrm{T}}SD - \frac{1}{2}\chi_{02}^{\mathrm{E}}D^2 \\ & -\frac{1}{6}\chi_{21}^{\mathrm{T}}S^3 - \frac{1}{2}\chi_{12}^{\mathrm{T}}S^2D - \frac{1}{2}\chi_{03}^{\mathrm{T}}SD^2 - \frac{1}{6}\chi_{03}^{\mathrm{E}}D^3 \end{aligned}, \quad (18)$$

where χ_{ij}^{T} and χ_{ij}^{E} are coefficients. Provided they are given, we can calculate V_{NE}=-LE_{N}, and V_{NT}=-$\beta^{\mathrm{S}}LT_{\mathrm{N}}/h$ after extracting proper frequency components from T_{N} and E_{N} in Eqs. (17) and (18) and substituting D and S determined by the linear analysis.

Finally, the nonlinear response is calculated by applying the peripheral circuits to the equivalent circuit shown in Fig. 5.

It should be noted that since equivalent circuits given in Figs. 3 and 5 will be used in different frequencies, their parameters are not necessary to be identical.

It is interesting that since D and S are spatially uniform, T_{N} and E_{N} are also uniform in addition to S_{N} and D_{N}.

III. Comparison Between Theory and Experiments

A. *Linear Simulation*

First, parameters in Fig. 3 are determined by fitting with the experimental data. Fig. 6 shows the measured input admittance of a FBAR with the Ru/AlN/Ru structure[12]. In the figure, the fitted result is also shown. It is seen that the agreement is excellent.

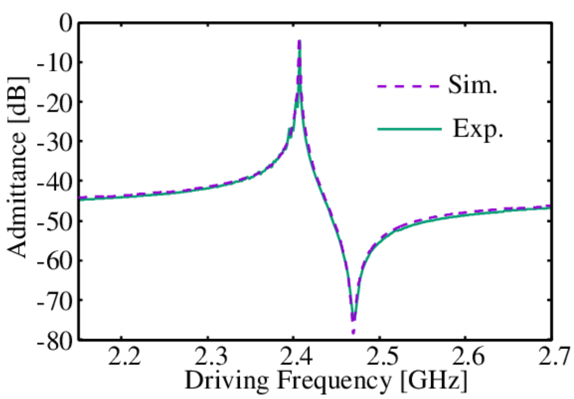

Fig. 6 Measured simulated admittance responses

B. *H2 Simulation*

Next, the second-harmonic (H2) response is analyzed by using equivalent circuit parameters determined by the above fitting.

Fig. 7 shows the measured result. A peaky response is seen, which indicates terms only including S^2 are dominant. Namely, S ($\propto I_{\mathrm{m}}$) exhibits a peaky dependence similar to the Bode Q[13], while D exhibits a notch at the anti-resonance frequency. H2 is almost constant at f < 2.25 GHz. This indicates that term(s) with D^2 also contribute to the output.

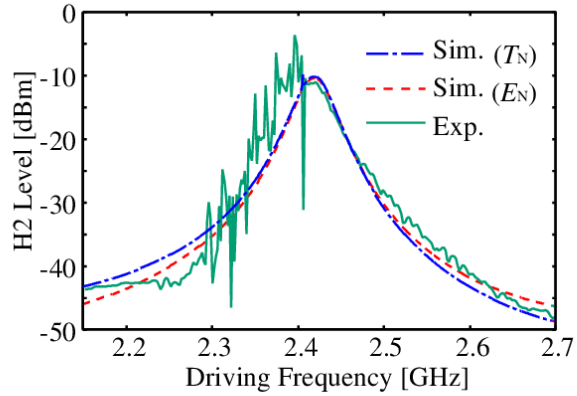

Fig. 7 Measured and simulated H2 responses

In the figure, two simulation results are shown: one considers $\chi_{20}^{\mathrm{T}}S^2$ and $\chi_{02}^{\mathrm{T}}D^2$ in T_{N} only while another does $\chi_{11}^{\mathrm{T}}S^2$ and $\chi_{02}^{\mathrm{E}}D^2$ in E_{N} only. Both results are quite similar to the experimental one, and it is hard to clarify which one is dominant.

Note strong spike trains are seen below the peak frequency. They are due to transverse mode resonances[7,14], and are not taken into account in the present 1D simulation.

The authors also simulated H2 response using the wave-equation based technique proposed in [6], and its result was quite similar to that shown in Fig. 7.

IV. Discussions and Conclusions

In this paper an equivalent circuit was derived for nonlinear responses in FBAR from the first-order perturbation analysis of the constitutive equations with h-form. In the derivation electrodes and piezoelectric layer are regarded as simple two masses and a spring, simplicity, for simplicity._Then it was demonstrated that the H2 response can be simulated well by the circuit. Although details are omitted due to page limitation, the authors verified that the current model is effective also for the H3 analysis.

The derived equivalent circuit indicates the followings:

When the driving frequency is far from the resonance, only terms proportional to D^n contribute to the output, which is almost independent of frequency. In contrast, when the driving frequency is close to the resonance, the other terms proportional to S^n also contribute. Terms only including S^n exhibit a peaky response. The other terms with S^nD^m are also peaky, but a notch appears at the anti-resonance frequency where D~0. Note that larger n makes the peak steeper.

When the driving frequency is chosen close to the resonance, the nonlinear response caused by T_{N} is hardly distinguishable with that caused by E_{N}. On the other hand, impacts of T_{N} and E_{N} are different when the resulting frequency is close to the resonance. For example, E_{N} will cause a dip in the nonlinear response when the resulting frequency is close to the anti-resonance one.

Note that the equivalent circuit proposed in this paper can be extended to cases including transverse mode resonances[15].

For SAW devices, notches are often observed in nonlinear responses when the driving frequency coincides with the resonance frequency instead of the anti-resonance one[3,4]. This means power series expansion should be given in a form of S^nE^m rather than S^nD^m. Namely, the constitutive equations with the *e* form seem better than those of the *h* form for the case.

ACKNOWLEDGMENT

The authors thank Dr. Ueda, Mr. Nishihara, Mr. Taniguchi, Mr. Iwaki and Mr. Irieda of Taiyo Yuden, Co. Ltd. for their fruitful discussions and supplying the measured data used in this paper. L.Qiu acknowledges financial support from Frontier Science Program of Graduate School of Science and Engineering, Chiba University. X. Li acknowledges the support of the Japanese Government (MEXT) for the scholarship through the Super Global University Project.

REFERENCES

[1] M.Ueda, M.Iwaki, T.Nishihara, Y.Satoh, and K.Hashimoto, “Nonlinear Distortion of Acoustic Devices for Radio-Frequency Front-End Circuit and Its Suppression,” Jpn. J. Appl. Phys., **49**, 7 (2010) 07HD12-1~5.

[2] D.S.Shim, and D.A.Feld, “A General Nonlinear Mason Model and Its Application to Piezoelectric Resonators,” International Journal of RF and Microwave Computer-Aided Engineering, 21, 5 (2011) pp. 486-495.

[3] R.Nakagawa, H.Kyoya, H.Shimizu, T.Kihara, and K.Hashimoto, “Study on Generation Mechanisms of Second-Order Non-linear Signals in SAW Devices and Their Suppression,” Jpn. J. Appl. Phys., **54**, 7 (2015) 07HD12-1~6.

[4] R.Nakagawa, T.Suzuki, H.Shimizu, H.Kyoya, K.Nako, and K.Hashimoto, “Discussion about Generation Mechanisms of Third-Order Nonlinear Signals in Surface Acoustic Wave Resonators on the Basis of Simulation,” Jpn. J. Appl. Phys., **55**, 7 (2016) 07KD02-1~7

[5] H.G.Brachtendorf, G.Welsch, and R.Laur, “Fast Simulation of the Steady-State of Circuits by the Harmonic Balance Technique,” Proc. International Symp. on Circuits and Systems (1995) 1388-1391.

[6] K.Hashimoto and X.Li, “Perturbation Analysis of Nonlinear Signal Generation in Radio Frequency Bulk Acoustic Wave Resonators,” Proc. IEEE Freq. Contr. Symp. (2017) 10.1109/FCS.2017.8088951

[7] L.Qiu, X.Li, N.Matsuoka, T.Omori, and K.Hashimoto, “Impact of Transverse Mode Resonances on Second Harmonic Generation in Radio Frequency Bulk Acoustic Wave Resonators,” Jpn. J. Appl. Phys., **58**, 7 (2019) SGGC02-1~5

[8] K.M.Lakin, J.Belsick, J.F.McDonald, and K.T.McCarron, “Improved Bulk Wave Resonator Coupling Coefficient for Wide Bandwidth Filters,” Proc. IEEE Ultrason. Symp. (2001) pp. 827-831.

[9] J.F.Rosenbaum, “10.5 Butterworth-Van Dyke Equivalent Circuit,” in Bulk Acoustic Wave Theory and Devices (Artech House, London, 1988) pp. 389-191.

[10] J.D.Larson, P.Bradley, S.Wartenberg, and R.C.Ruby, “Modified Butterworth-Van Dyke Circuit for FBAR Resonators and Automated Measurement System,” Proc. IEEE Ultrason. Symp. (2000) pp. 863-868.

[11] B.A.Auld, “Thermodynamics of Solids,” in Acoustic Fields and Waves in Solids, Second Edition, Vol. 1 (Klinger, Malabar, FL, USA, 1990) pp. 275-280.

[12] S.Taniguchi, T.Yokoyama, M.Iwaki, T.Nishihara, M.Ueda and Y.Satoh, “An Air-Gap Type FBAR Filter Fabricated Using a Thin Sacrificed Layer on a Flat Substrate,” Proc. IEEE Ultrason. Symp. (2007) pp. 600-603

[13] D.A.Feld, R.Parker, R.Ruby, P.Bradley, and S.Dong, “After 60 Years: A New Formula for Computing Quality Factor is Warranted,” IEEE Ultrason. Symp. (2008) pp. 431-436.

[14] T.Yang, Z.Cao, and D.Feld, “An H2 emission model for piezoelectric devices exhibiting strong lateral mode resonances,” Proc. IEEE Ultrason. Symp. (2017) 10.1109/ULTSYM.2017.8092136

[15] L.Qiu, X.Li, T.Omori, and K.Hashimoto, “Mechanism of Enlarged Nonlinear H2 Response by Transverse Modes in RF BAW Devices,” Proc. USE2019 (2019) [to be published]